ELM characteristics and divertor loads in ASDEX Upgrade helium discharges

A. Scarabosio *, C. Fuchs, A. Herrmann,

E. Wolfrum and the ASDEX Upgrade Team

Max-Planck-Institut für Plasmaphysik, EURATOM-Association, Boltzmannstr. 2, D-85748, Garching, Germany

Abstract

Discharges with helium as working gas are the best candidate for reaching the ELMy H-mode regime during the non-nuclear phase in ITER. It is extremely important to explore the ITER tokamak physics and ELM mitigation techniques before the nuclear phase. Yet, little is known on the ELM regime and target loads expected in He plasmas close to L-H power threshold and with a large fraction of tungsten material in the divertor. In this contribution we analyse the ELM characteristics in a set of ASDEX Upgrade He H-mode pulses with carbon and tungsten target tiles. We find that both larger type-I-like and smaller type-III-like ELM can be obtained similar to the D case. With tungsten, and in contrast with carbon target, we observe no reversal in the thermal loads asymmetry during ELM, which is always larger at the outer target. The fraction of the ELM energy loss reaching the target tend, for higher losses, to become smaller in D discharge than in He, probably due to different radiation pattern.

Key words: ASDEX-Upgrade, Edge plasma, Divertor, ELM

PACS: 52.25.Ya, 52.55.Fa, 52.25.-b

1 Introduction

At present the predictions for Edge Localised Modes (ELM) related phenomena in ITER, such as the maximum power loads to the targets due to ELM losses, spatial distribution of losses, etc..., are still highly uncertain [1]. However, this knowledge is of particular concern for ITER (especially for large ELMs of type I) in order to address a number of edge plasma/divertor physics and technical issues as ELM pacing and mitigation techniques. Given the rather different edge/divertor plasma conditions expected for ITER it is also not clear whether precise enough predictions can be obtained from experiments on present day machines. Therefore achieving the high confinement regime (H-mode) during the non-nuclear phase of ITER in hydrogen or helium plasmas is highly desirable. The power threshold (P_{thr}) for reaching the H-mode in hydrogen is typically about 2 times larger than in deuterium [2] making this scenario very unfavourable due to the limited external heating power available. In contrast, it has been shown in JET [3] that P_{thr} in helium is only 40% higher than in D and very recent experiments in ASDEX Upgrade (AUG) in 2008 [4] have found no difference in P_{thr} between He and D plasmas. This, of course, makes the use of helium very attractive for ITER.

It is not yet clear, however, if the physic of ELMs and the energy loss mech-

* Max-Planck-Institut für Plasmaphysik, EURATOM-Association, Boltzmannstr. 2, D-85748, Garching, Germany
Email address: andrea.scarabosio@ipp.mpg.de.

anisms are similar for He and D and thus whether a direct extrapolation to D-D or the D-T phase from ITER He discharges is possible. Also plasma conditions may be too different since the expected total heating power is close to the L-H threshold in He but well above in D. In this work we investigate the ELM characteristics and their influence of the divertor target loads in He discharges on AUG and compare them with similar discharges in D in in view of the possibility of extrapolating from He to D plasmas in ITER. The 2008 AUG He discharges [4] together with older experimental data are used as database. The older discharges were heated with deuterium neutral beam injection (D-NBI) and had carbon target tiles. The 2008 pulses are heated with H-NBI and/or ECRH, and have a tungsten coated target tiles. The first wall is W in all cases. We point out that these newer experiments are the first with full tungsten first wall and divertor, thus very important in view of the increasing fraction of tungsten for the foreseen ITER divertor. The main plasma parameters, namely plasma current, magnetic field, line averaged density, total heating power, safety factor and plasma triangularity range respectively between I_p=0.6-1MA, B_T=1.5-3T, $\bar{n}_e$=3.6-9.1e19m^{-3}, P_{tot}=1.7-6.5MW, q_{95}=3.1-5.1 and δ=0.14-0.28. The He content, $n_{He}/(n_{He} + n_{H(D)})$, is up to about 75% in pure ECRH heated discharges and lower with NBI. The database and the experiments are described in more details in [4]. Particular emphasis is given here to plasmas with input power marginally above the P_{thr}, a condition to be expected in ITER He-plasmas. As already mentioned, an early important result from the 2008 He discharges, in contrast to previous data, was the finding of an L-H transition threshold power similar than in D. The energy confinement in H-mode was about 0.75 that an equivalent D discharges [4], mainly due to ion dilution because of $Z_{He} = 2$. We note that the use of helium precluded efficient divertor cryogenic pumping (unlike in

companion D pulses) resulting in a poor density control.

1.1 ELM observation and methodology

ELMs appear as clearly defined peaks on many measurements such as divertor currents, Mirnov coils, W influx, recycling fluxes and target surface temperature (see figure 1). At AUG these are commonly used as 'ELM monitors'. In particular, the fast and high quality divertor current signals provide good a reference to identify the start, $\tau_{ELM,s}$, and the end, $\tau_{ELM,e}$, of each individual ELM event. Based on these times, the ELM frequency, the ELM losses and all other ELM related quantities are calculated. Total radiated power is given by a standard foil bolometer, plasma energy is taken from the equilibrium reconstruction and thermal load in the divertor are measured with infrared cameras (IR) covering both inner and outer target tiles. Details on the IR system can be found in [5]. Heat fluxes on the target are calculated from IR temperature evolution using the THEODOR code [5]. Integration of the power flux density poloidally along the targets gives the total power from which then the energy reaching the divertor is computed under the assumption of toroidal symmetry. Since the decay of the power signal after the maximum is found experimentally to be longer than the decay of the divertor currents (see section 3), $\tau_{ELM,e}$ is extended by 3ms for all discharges analysed for a total ELM time window of 4-6ms (shaded area in figure 1). This limits a meaningful analysis of the target loads to ELM with frequency below 150Hz, typically the larger ELM in the database.

2 Identification and characteristics of ELMs in He

In He discharges at AUG we find two different types of ELMs. The first has frequency between f_{ELM}=25-200Hz and relatively large crashes in the plasma energy. An example of the first type of ELM is shown in figure 2a). The frequency increases from 100Hz to 150-180Hz at the last power step showing type-I behaviour (following the standard classification of ELMs according to the power dependence of f_{ELM} [6]). The second type of ELM encountered has generally higher f_{ELM} (200-500Hz) which decreases with heating power and often exhibits smaller peaks in the ELM's monitors than the first type. The NBI power ramp up in figure 2b) causes an increase of the divertor current peaks and a monotonic decrease of f_{ELM}. This ELM type is thus identified as type-III. We note that the power dependence of this type-III ELM is the same as for D plasmas but opposite to what it is found in JET He plasmas for small and frequent ELMs [3]. In many discharges of the database, the direct identification of the ELM's type (through power dependence) is complicated by the simultaneous variation of the plasma density (and thus the associated fueling and recycling level), which was not controlled during the H-mode phase. Therefore the ELM type could be clearly identified only in a limited number of discharges. In order to attempt a rough identification, we plot f_{ELM} versus P_{tot} normalised to the L-H power threshold scaling $P_{thr} = 0.049 B_T^{0.8} n_{20}^{0.72} S^{0.94}$ [7,4] (figure 3). The ELM frequencies and heating powers are averaged over stationary phases of the discharges. Although these two parameters alone are by no means sufficient to order ELMs we note, however, that there is a tendency for the type-I and in general for low frequency ELMs to appear at higher P_{tot} whereas the type-III are more common at low P_{tot}/P_{thr}. Also, at

lower I_p, only type-I are observed with f_{ELM} clearly increasing with P_{tot}/P_{thr}. Based of the experimental scaling, this occurrence can be explained by the lower B_T applied to keep similar edge safety factor as for higher I_p. At intermediate P_{tot}/P_{thr} we report the existence of discharges with both low and high frequency ELMs and cases where sharp transitions between the two frequency ranges are observed. The pure ECRH heated plasmas tends to have type-III ELM of even smaller, below detection limit. This may be due to the limited power available $P_{ECH} \leq 2.1$MW. Finally we note that in D plasmas, at the same P_{tot}/P_{thr}, f_{ELM} is at in the lower boundary of the He plasmas, thus appearing to enter the type-I regime somewhat more easily. This fact may be qualitatively justified by the higher pedestal pressure gradient in D H-mode under these conditions and thus by the larger ideal drive of the MHD instability (i.e. pressure drives vs. current driven ELMs).

3 Energy losses and divertor loads

3.1 Main plasma losses

The ELM energy losses ΔW_{loss} from the equilibrium reconstruction are calculated for each ELM during stationary phases of the discharge for the available database. We then take the mean value for ΔW_{loss} and the standard deviation as estimator of its error. The standard deviation (which includes the statistical errors plus the intrinsic variation of ΔW_{loss} mainly due to variation of the ELM cycle ie. of f_{ELM}) ranges from 100-200% for $\Delta W_{loss} \leq 5$kJ to down to 15-30% for $\Delta W_{loss} \geq 20$kJ. The largest ELM loss in the database is 34kJ. It has been shown for ASDEX Upgrade and JET Deuterium plasmas a link be-

tween the fraction of ELM energy loss and the ELM period $\tau_{ELM}(\equiv 1/f_{ELM})$ normalised to the energy confinement time τ_E, ie. $\Delta W_{loss}/W_{MHD} \propto \tau_{ELM}/\tau_E$ [8,9]. Figure 4 shows a quite good correlation of 85% of $\Delta W_{loss}/W_{MHD}$ with τ_{ELM}/τ_E. Both type-I and type-III ELMs are plotted. At low I_p, up to 11% of the plasma energy can be lost during a single ELM. Importantly, the fraction of ELM energy losses in similar D plasmas lies in the same range and seems to scale similarly with τ_{ELM}/τ_E, despite the difference in confinement time and energy content (mainly due to ion dilution $W_i(He) =\simeq 0.5 W_i(D)$ [4]). If fact, the longer confinement time in D (for the same P_{tot}) is compensated by the larger W_{MHD} resulting in a similar scaling. This may indicate that the ELM affected area and loss dynamic (i.e. MHD mode characteristics) are similar for D and He for the same plasma conditions. The fraction of ELM power loss $P_{ELM}(\equiv f_{ELM} \cdot \Delta W_{loss})/P_{tot}$ ranges between 10-60% in He and 10-40% for D for similar heating scheme, where the highest P_{ELM}/P_{tot} values are reached for type-III ELMy discharges. The power loss fraction does not appear to depend strongly on P_{tot}, I_p or Greenwald fraction.

3.2 Divertor target loads during type-I ELM in He

We compare target temperature profiles at the maximum and minimum of the ELM cycles, averaging the profile over all ELMs. Examples of such averaged profile for two similar He discharges with CFC and W target is shown in figure 5. Thermal loads during ELM have changed dramatically with the W divertor: the inner target temperature increase is strongly reduced by approximately a factor of 5 whilst the outer target load remains similar. The derived power fluxes are thus much lower at the inner target and never exceed $10\mathrm{MW}/m^2$ for

$P_{tot,max}$=6.5MW. The power integrated over the target is smaller by a similar factor. Under these conditions, the outer target sees during ELMs higher power density than the inner target, contrary to what is normally observed with carbon target in ASDEX Upgrade and other tokamaks. In between ELMs, the power is also larger at the outer target thus not showing the reversal loads asymmetry as for carbon targets. The larger power loads at the outer W-target can be clearly seen in figure 6 where we compile the maximal heat flux density during ELM for three different pulses in He and in D. The low power at the inner divertor appears to be a general feature not only in He but also in D plasmas, and it does not depend upon whether the inner target is power attached or detached in the inter-ELM phase. Part of the difference is surely due to the higher and differently distributed plasma radiation with W. Diagnostic issues such as reflection and/or surface layers may influence the IR measurements but are unlikely to change the main features of the observations. In the following we focus mainly on the comparison of He and D and we leave the detailed analysis of the effect of high-Z material on the thermal loads for future work.

The shape of the power flux density profile on the target is similar for both working gases, perhaps only slightly narrower in He as shown in 6. For the same plasma energy loss, more the power peak at the targets are larger in He than in D but perhaps the profiles are somewhat narrower. More data and analysis are needed to clarify if the ELM wetted area is similar in the two cases. We have then investigated the relation between ΔW_{loss} and ΔW_{IR}, the total thermal energy reaching tungsten targets. ΔW_{IR} is calculated from the total power flux in a time window similar that in figure 1 (4-6ms) and then averaged over many ELMs in a similar fashion as for ΔW_{loss}. ΔW_{IR} is

not corrected for the background power arriving during this relatively long time window. In He we find $\Delta W_{loss} \approx \Delta W_{IR}$ whereas in D, at least for the highest energy loss, $\Delta W_{loss} \geq \Delta W_{IR}$ (figure 7 and table 1). This finding is partly in contradiction with reference [9] in which $\Delta W_{target} \approx 0.5 \Delta W_{loss}$ was obtained. In [9], however, larger ELM size with CFC target were considered. This difference between He and D can be explained, in the few cases studied here, by a larger fraction of radiated power. In fact the degree of power balance, $(\Delta W_{ELM} + P_{tot}\Delta t)/(\Delta W_{IR} + \int_0^{\Delta t} P_{rad} dt)$, is similar similar for D and He due to enhanced P_{rad} as indicated, for few discharges only, in table 1. The fraction of missing power is similar to what found in previous studies, ranges from 0 to 30% and suggests that a non-negligible amount of power goes to the first wall. This missing power is also often larger for the ELM phase than the inter-ELM phase.

4 Summary and discussion

In summary, in helium H-mode discharges on AUG we observe similar ELM phenomenology as in deuterium showing both type-I and type-III like behaviour. A larger heating power in He than in D seems to be needed to enter reliably the type-I regime. The fraction of ELM energy losses lies in the same range and scale similarly with global confinement time and ELM frequency. These results on AUG indicate that type-I ELM regime in helium is reached with $P_{tot}/P(He)_{thr} \geq 1.5$. Assuming for ITER about 70-80MW available for heating and the predicted $P(D)_{thr} = 53MW$ [7], type-I ELM may be reached at full current only if $P(He)_{thr} \approx P(D)_{thr}$ as seen for AUG [4]. In this case a number of technical and physics issues related with ELMs may be addressed

on ITER during the helium non-nuclear phase. If the L-H power threshold is considerably higher as in JET, [3] type-I ELM in helium may be still obtained at reduced plasma current. Large uncertainties on these conclusions arise from level of purity in the He discharges obtained so far on AUG, which is always below 75%. This may in fact play a key role for the differences observed with JET experiments in L-H threshold and ELM behaviour. Also, it would be interesting to repeat and expand the database with experiments with the higher plasma triangularity foreseen for ITER and higher ECRH power as now available on ASDEX Upgrade.

References

[1] A. Loarte et al., Physics of Plasmas, 11 (2004), 2668

[2] E. Righi et al., Nucl. Fusion, 39 (1999) 309-319

[3] D. C. McDonald et al.,Plasma Phys. and Controlled Fusion 46 (2004) 519-534

[4] F. Ryter et al., Nucl. Fusion, 49 (2009) 062003

[5] A. Hermann et al., Plasma Phys. and Control Fusion, 37 (1995)

[6] H. Zohm et al., Nucl. Fusion, 38 (1996) 105-128

[7] Y.R. Martin et al., J. Phys.:Conf. Ser. (2008) 123 012033

[8] H. Urano et al., Plasma Phys. and Control. Fusion, 45 (2003) 1571-1596

[9] A. Hermann et al., J. Nuclear Mater., (2003) 313-316, 759

5 Figure captions

Fig. 1. ELM monitors from top to bottom: inner and outer divertor currents, surface temperature at outer target, H_α radiation in the outer divertor, neutral fluxes in the divertor, MHD plasma energy. The start and end of an ELM based on the divertor current diagnostic are indicated with arrows and a typical window for the IR data analysis with a shaded area.

Fig. 2. From top to bottom the signals shown are time traces of total heating power, divertor currents and derived ELM frequency. a) 0.6MA/-1.5T He discharge (#23602) showing type-I ELM behaviour. b)1MA/-2T He discharge (#23609) showing type-III ELM behaviour.

Fig. 3. ELM frequency versus total heating power, scaled to the Deuterium L-H transition power for the full database of He ELMy discharges. The data points are classified according to their power dependence and plasma current. Circles are for the 'not identified' type, square symbols are type-I, diamonds mixed type, triangles type-III. Blues symbols are 1MA discharges and red symbols 0.6MA.

Fig. 4. Energy loss fraction as a function of the ELM period normalised to the energy confinement time for discharges with δ >0.2 The error bars only contain estimate for W_{loss}, error in the other quantity are neglected. The linear fit is shown with a dashed black line.

6 Table caption

Fig. 5. Maximal (dashed line) and minimal (full line) temperature profiles along the target from inner to outer during the ELM cycle. He plasmas with CFC a) and W b) target material. The two plasma are LSN with similar shape heated with 4.5MW D-NBI and 5MW H-NBI respectively.

Fig. 6. Maximal power flux profile averaged over many ELMs for a He plasma (full line) and two D plasmas (dashed and dot-dashed lines) with different ELM size.

Fig. 7. ELM energy to the target versus plasma energy loss in He (circles) and D (squares) for discharges with $f_{ELM} > 150$Hz.

Table 1

Inter-ELM and ELM power balance for discharges with tungsten divertor in helium and deuterium. The ELM loos, the target load, the gas type, the total input pwer and the number averaged ELM are also tabulated.

7 Figures

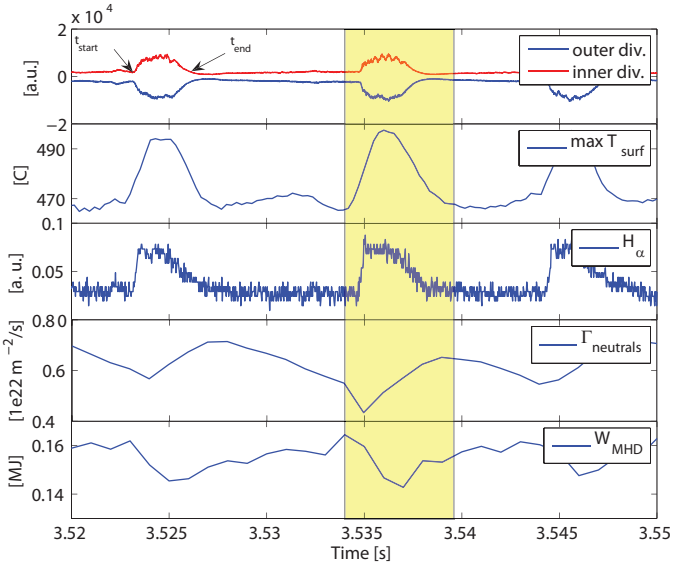

Figure 1

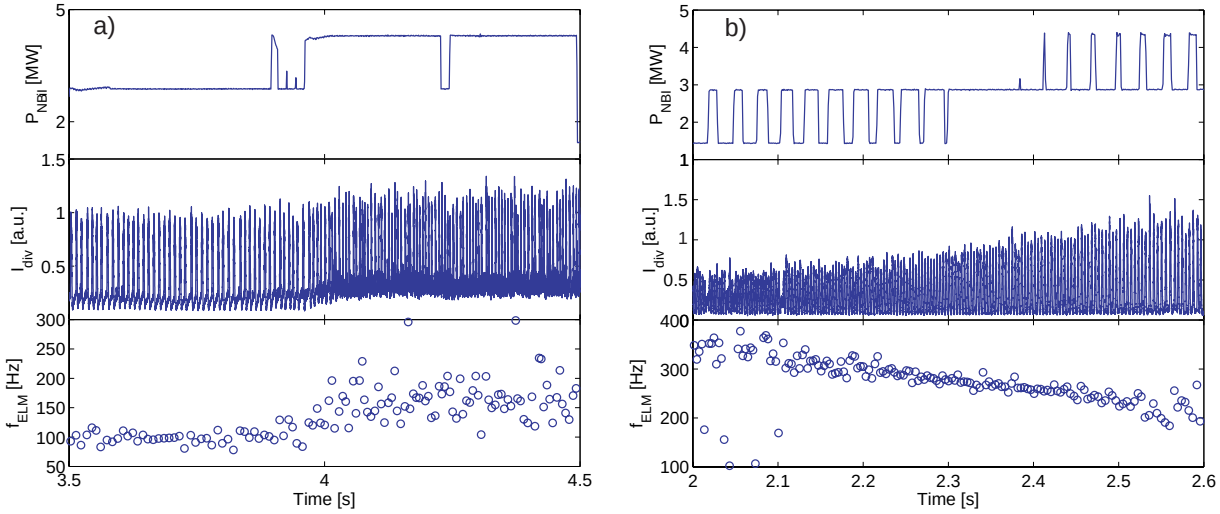

Figure 2

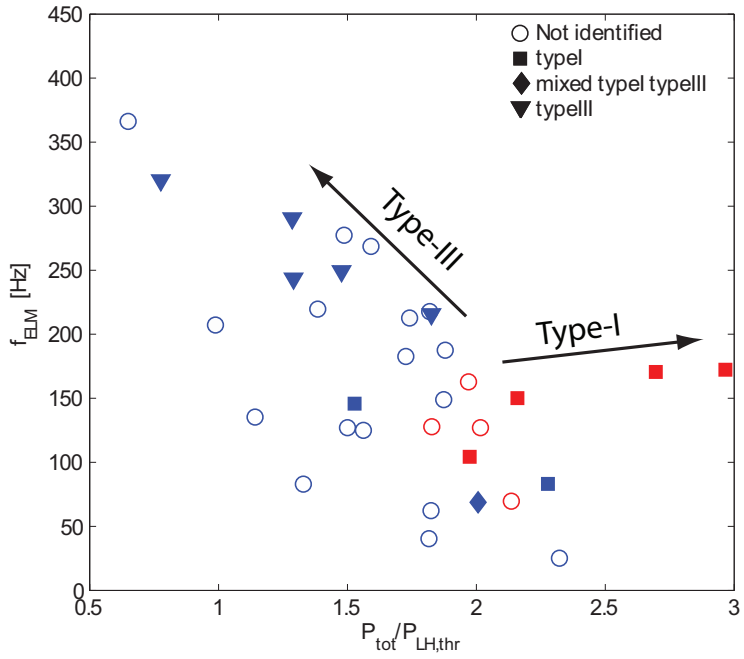

Figure 3

8 Tables

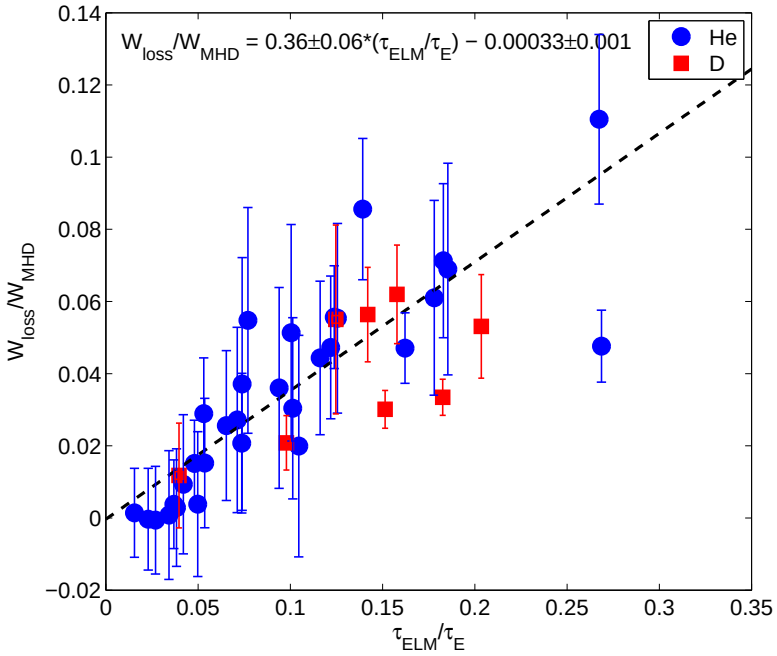

Figure 4

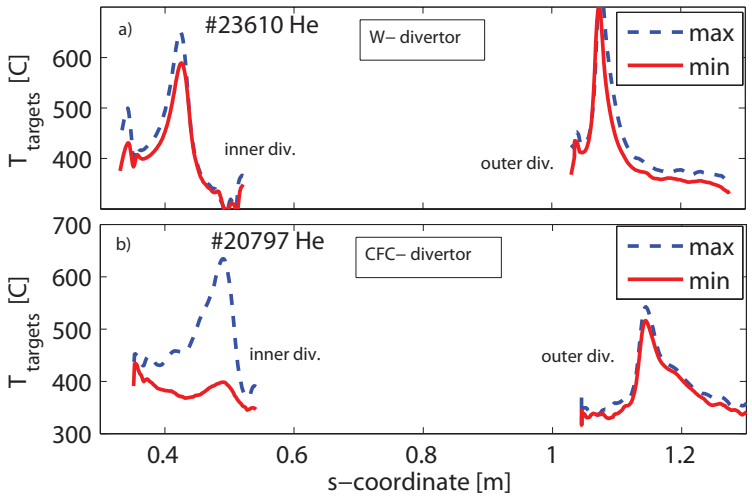

Figure 5

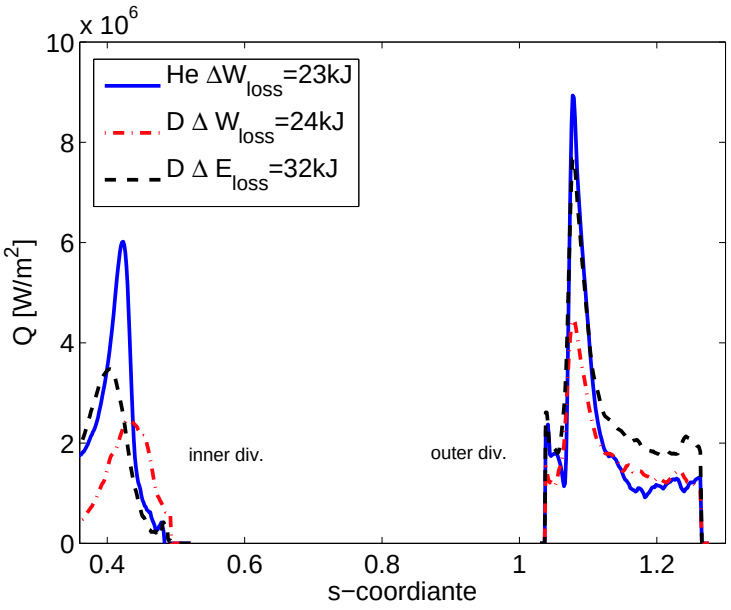

Figure 6

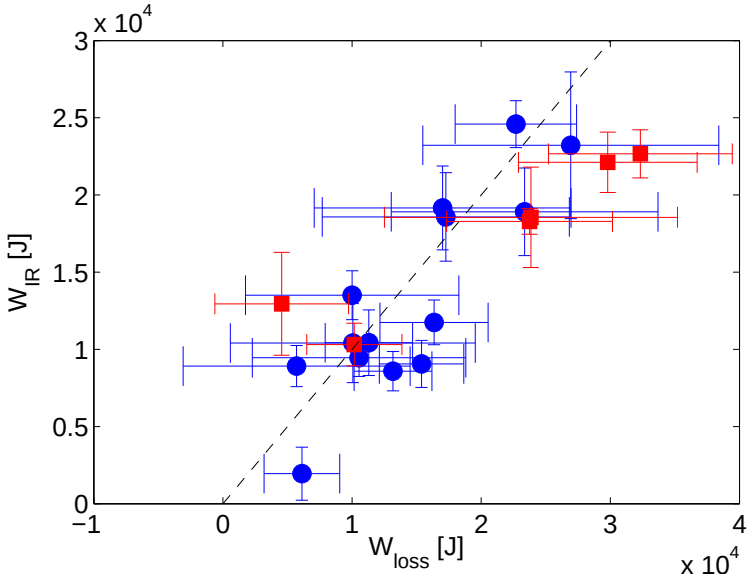

Figure 7

Table 1

SHOT #	gas	$P_{bal,int-ELM}$	$P_{bal,ELM}$	ΔW_{IR} [kJ]	ΔW_{ELM} [kJ]	P_{tot} [MW]	n. ELM
23603	He	0.76	0.67	18.6	17.3	4.9	53
23610	He	0.81	0.83	24.6	22.7	6.5	17
23795	D	1.01	0.90	18.6	24.0	3.3	21
24097	D	0.70	0.72	22.7	32.3	5.4	27